

ZERODUR[®] and OPTICAL GLASS

in High-Stress Applications

Peter Hartmann

SPIE PRESS
Bellingham, Washington USA

Library of Congress Cataloging-in-Publication Data

Names: Hartmann, Peter (Optical engineer), author. | SPIE (Society), issuing body.
Title: ZERODUR and optical glass in high-stress applications / Peter Hartmann.
Other titles: Optical glass in high-stress applications.
Description: Bellingham, Washington, USA : SPIE, [2024] | Includes bibliographical references and index.
Identifiers: LCCN 2024025316 | ISBN 9781510679894 (paperback) | ISBN9781510679900 (pdf) | ISBN 9781510679917 (epub)
Subjects: LCSH: Registration symbol after “ZERODUR” on title page. | Optical glass–Testing. | Optical glass–Mechanical properties. | Optical glass–Expansion and contraction. | Optical glass–Deterioration. | Brand name products.
Classification: LCC QC375 .H28 2024 | DDC 666/.156–dc23/eng20240720
LC record available at <https://lcn.loc.gov/2024025316>

Published by
SPIE
P.O. Box 10
Bellingham, Washington 98227-0010 USA
Phone: +1 360.676.3290
Fax: +1 360.647.1445
Email: books@spie.org
Web: www.spie.org

Copyright © 2024 Society of Photo-Optical Instrumentation Engineers (SPIE)

All rights reserved. No part of this publication may be reproduced or distributed in any form or by any means without written permission of the publisher.

The content of this book reflects the work and thought of the author. Every effort has been made to publish reliable and accurate information herein, but the publisher is not responsible for the validity of the information or for any outcomes resulting from reliance thereon.

Printed in the United States of America.

First printing 2024.

For updates to this book, visit <http://spie.org> and type “PM378” in the search field.

SPIE.

Contents

| | |
|---|-------------|
| <i>Preface</i> | <i>ix</i> |
| <i>Acknowledgments</i> | <i>xi</i> |
| <i>Historical Background and Overview</i> | <i>xiii</i> |
| 1 Mechanical Strength of Glass: Introduction | 1 |
| 1.1 Application Cases and Related Questions | 1 |
| 1.2 Breakage Condition | 3 |
| 1.3 Ideal versus Practical Strength | 4 |
| 1.4 Surface Condition: Micro-cracks | 5 |
| 1.5 Bending Strength | 9 |
| 1.6 Deterministic Fracture Mechanics | 10 |
| 1.7 Statistical Breakage Probability Distribution | 11 |
| 1.8 Fatigue-Dependent Breakage Threshold Stress | 11 |
| 1.9 Fatigue | 12 |
| 1.10 Risk Considerations | 12 |
| 1.11 Compressive Stress | 13 |
| Further Reading | 14 |
| References | 14 |
| 2 Breakage Stress Measurement | 17 |
| 2.1 General | 17 |
| 2.2 Surface Conditions | 18 |
| 2.3 Specimen Preparation and Pre-inspection | 20 |
| 2.4 Measurement Setup: Ring-on-Ring Method | 23 |
| 2.5 Measurement Setup: Four-Edge Method | 28 |
| References | 29 |
| 3 Evaluation of Measurements: Weibull Distribution | 31 |
| 3.1 General | 31 |
| 3.2 The Weibull Extreme Value Statistical Distribution | 36 |
| 3.3 Weibull Plot | 36 |
| 3.4 Two- or Three-Parameter Weibull Distribution? | 38 |
| 3.5 Large-Size Breakage Stress Samples: Phenomenology | 42 |
| 3.5.1 Areal breakage stress non-uniformity | 43 |
| 3.5.2 Outliers | 45 |

| | | |
|----------|---|-----------|
| 3.6 | Threshold Stress Determination | 48 |
| 3.7 | Area Dependence | 49 |
| 3.8 | Application of the Three-Parameter Weibull Distribution and Its Limits | 51 |
| | References | 52 |
| 4 | ZERODUR®: Strength of Ground Surfaces | 53 |
| 4.1 | Introduction | 53 |
| 4.2 | Surface Conditions | 54 |
| 4.3 | ZERODUR® Ground with D151 Bonded Diamond Grains | 56 |
| 4.4 | Measurement Reproducibility | 57 |
| 4.5 | ZERODUR® Ground with D64 Bonded Diamond Grains | 58 |
| 4.6 | ZERODUR® Ground with D46, D35, and D25, Lapped with SIC 320 and SIC 600, and Optically Polished | 62 |
| 4.7 | Breakage Stress at Cryogenic Temperature | 65 |
| 4.8 | Conclusion | 65 |
| | References | 68 |
| 5 | Micro-crack Depths | 71 |
| 5.1 | Introduction | 71 |
| 5.2 | Micro-crack Depth Measurement Methods | 73 |
| 5.3 | Micro-crack Appearance | 74 |
| 5.4 | Micro-crack Depth Distributions of Ground and Lapped ZERODUR® Surfaces | 75 |
| 5.5 | Maximum Crack Depth | 78 |
| 5.6 | Threshold Stress and Maximum Crack Depth | 81 |
| | References | 83 |
| 6 | Bending Strength of Etched ZERODUR® | 85 |
| 6.1 | Introduction | 85 |
| 6.2 | Specimen Preparation | 87 |
| 6.3 | Ring-on-Ring Test Setup | 88 |
| 6.4 | Evaluation | 88 |
| 6.5 | Micro-cracks Change with Etching | 88 |
| 6.6 | Measurement Results for D151-Pre-ground ZERODUR® | 91 |
| 6.7 | Measurement Results for D64-Pre-ground ZERODUR® | 94 |
| 6.8 | Comparison of Etched Samples Pre-ground with D151 and D64 | 96 |
| 6.9 | Outliers | 97 |
| 6.10 | Stress Concentrations | 99 |
| 6.11 | Minimum Breakage Stress of Etched ZERODUR® | 103 |
| 6.12 | Recommendations for Highest Strength with Etching | 104 |
| 6.13 | Compilation of Experimental Data | 105 |
| | References | 106 |

| | | |
|----------|---|------------|
| 7 | Strength Change with Time: Fatigue | 107 |
| 7.1 | Fatigue Mechanisms: Wear and Stress Corrosion | 107 |
| 7.2 | Subcritical Crack Growth: Stress Corrosion | 107 |
| 7.3 | Measurement of the Stress Corrosion Constant | 109 |
| 7.4 | Derivation of the Stress Corrosion Constant versus Stress Increase Rate Equation | 110 |
| 7.5 | Stress Corrosion Constant Measurement: SCHOTT Results of 2010 | 111 |
| 7.6 | Stress Corrosion Constant Measurement: SCHOTT and Fraunhofer Institute Results of 2014 | 112 |
| 7.7 | Stress Corrosion Constant Measurement: All Measurements and Evaluation | 114 |
| 7.8 | Humidity: Influence on Strength During Storage without Stress Loads | 116 |
| | References | 118 |
| 8 | Design Strength of ZERODUR® Including Fatigue: Lifetime | 121 |
| 8.1 | Introduction | 121 |
| 8.2 | Lifetime Calculation with the Weibull Threshold Stress Model | 122 |
| 8.3 | Practical Application of the Model | 125 |
| 8.4 | Mechanical Loads Varying in Time | 127 |
| 8.5 | Lifetime Calculation: Test of the Model | 129 |
| | References | 133 |
| 9 | Bending Strength of Optical Glasses | 135 |
| 9.1 | Introduction | 135 |
| 9.2 | Bending Strength Dependence on Surface Conditions | 136 |
| 9.3 | Micro-cracks in Optical Glass | 138 |
| 9.4 | Breakage Stress Measurement Method | 140 |
| 9.5 | Breakage Stress Measurement Evaluations | 143 |
| 9.6 | Choice of Optical Glass Types for Breakage Tests | 144 |
| 9.7 | Breakage Test Results: Optical Glass Types—Overview | 146 |
| 9.8 | Breakage Test Results: Optical Glass Types—3 PW Fits | 147 |
| 9.9 | Breakage Test Results: Infrared-Transmitting, Color Filter, and Technical Glass Types—3 PW Fits | 149 |
| 9.10 | Breakage Test Results: Optical Flint Glass Types | 150 |
| 9.11 | Breakage Test Results: Lanthanum Optical Glass Types | 153 |
| 9.12 | Breakage Test Results: Miscellaneous Optical Glass Types | 154 |
| 9.13 | Breakage Test Results: Filter, Infrared Glass Types, and Technical Glasses | 156 |
| 9.14 | Breakage Test Results: Etched and Polished Samples | 157 |
| 9.15 | Breakage Stress Threshold: Correlation with Knoop Hardness and Young's Modulus | 158 |
| 9.16 | Fracture Toughness | 162 |

| | | |
|-----------|---|------------|
| 9.17 | Lifetime Prediction for Optical Glass Components under Tensile Stress Loads | 167 |
| 9.18 | Stress Data Compilation for Optical, Color Filter, Infrared, and Technical Glass Types | 172 |
| | References | 177 |
| 10 | Recommendations for Optimizing and Maintaining the Strength of Glass Items | 179 |
| 10.1 | Introduction | 179 |
| 10.2 | Risk Considerations | 179 |
| 10.3 | Strength Increase Methods | 181 |
| 10.3.1 | Grinding with smaller sized grains and reduced efficiency | 181 |
| 10.3.2 | Prestressing | 181 |
| 10.3.3 | Surface refinement | 183 |
| 10.4 | Design of a Glass Item to Reduce Breakage Probability | 183 |
| 10.5 | Design of Frames or Support Structures of Glass Elements to Reduce Breakage Probability | 184 |
| 10.6 | Maintaining Strength and Avoiding Unnecessary Strength Reduction | 185 |
| 10.7 | Repair | 185 |
| | References | 186 |
| 11 | Application Examples | 187 |
| 11.1 | Overview | 187 |
| 11.2 | X-ray Satellite ROSAT | 187 |
| 11.3 | X-ray Satellite AXAF/CHANDRA | 188 |
| 11.4 | LISA Pathfinder Satellite | 189 |
| 11.5 | KECK Telescopes | 191 |
| 11.6 | ESO ELT Extremely Large Telescope | 193 |
| 11.7 | Airborne Infrared Observatory SOFIA | 196 |
| | References | 196 |
| | <i>Index</i> | 199 |

Historical Background and Overview

The first in-depth mechanical strength analysis of the extremely low-expansion glass ceramic ZERODUR[®] was made by SCHOTT AG, Germany, together with the company Dornier, Friedrichshafen, Germany, and the Fraunhofer Institute for Mechanics of Materials (IWM) in 1983. The purpose was to assess its suitability for use with the German x-ray satellite ROSAT. This work remained unpublished. In 1989, the next investigation took place on the occasion of the NASA x-ray satellite CHANDRA, at that time, still with its preliminary name AXAF. Its large, thin, hollow ZERODUR[®] shells needed to survive the space shuttle launch. The acting forces were not very high because this was a manned space mission.

In 2007, strength research with ZERODUR[®] began again. This time the reason was the intended use of ZERODUR[®] for structural elements of LISA Pathfinder, the ESA gravitational antenna precursor satellite. The elements needed to withstand considerably higher forces during the launch, which was performed with an unmanned rocket. The research that started with this project and that was later continued led to considerable progress in high-stress applications of ZERODUR[®].

The strength of brittle glass and glass ceramic materials depends exclusively on their actual surface condition and the environmental media, especially humidity. In all practical surfaces, there are small cracks that will grow when tensile stresses at their locations exceed a minimum value. With ever increasing stress, the growth will accelerate until it reaches its final speed and breakage occurs. As long as the tensile stress remains at values only slightly above the growth threshold, and with the cracks being small, their growth will be very slow, and the glass item will remain intact for a long time. This so-called subcritical crack growth follows a law that allows one to calculate the time until breakage.

Unfortunately, not only does crack growth depend exponentially on the crack's initial length, but the exponent is a large number. Slight length changes result in very largely differing growth speeds. This can easily amount to several orders of magnitude. Critical applications cannot accept lifetime span predictions with uncertainty ranging from minutes to years and therefore

Chapter 1

Mechanical Strength of Glass: Introduction

1.1 Application Cases and Related Questions

The ultralow-expansion glass ceramic ZERODUR[®] finds more and more applications with higher mechanical loads:¹⁻⁵

- Large thin mirrors with high diameter-to-thickness ratio ($\gg 6:1$). An outstanding example is the 4.25-m mirror of the U.S. Daniel K. Inouye Solar Telescope [DKIST, formerly called the Advanced Technology Solar Telescope (ATST)] with a 70-mm thickness being tilted in operation beyond 90 deg with respect to the horizontal position.⁶
- Filigree lightweight mirrors and structures⁷ that must survive strong forces when being launched to space [see Fig. 1.1 (*left*)]. This holds for the high-precision frames and optical bench of the gravitational research satellite LISA Pathfinder, for example [see Fig. 1.1 (*right*)].

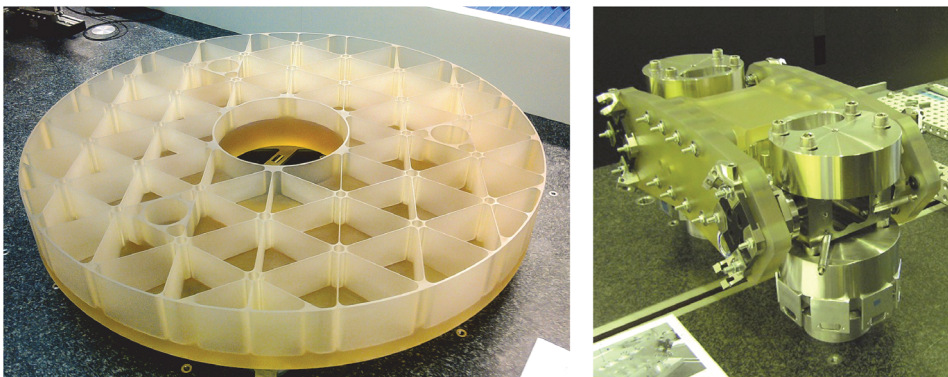


Figure 1.1 (*left*) 1.2-m ZERODUR[®] lightweight mirror with 2-mm ribs on the back side (photo credit: SCHOTT AG). (*right*) Prototype frame structure of the LISA Pathfinder satellite clamping metal masses. The flight model was launched successfully in Dec. 2015 (reprinted from Ref. 24).

instantaneous breakage. Only when the micro-cracks grow deeper with further stress increase and their depths surpass a limit value will breakage occur.

Up to high-stress values, metals do not show considerable statistical variations in strength. Such variations will occur at stress levels that are higher than designed in any application. For brittle materials, however, purely statistical behavior is assumed. This means that even at a very low stress level, the failure probability is still different from zero. In the framework of the investigation outlined in this book, it has been shown that for glass and glass ceramics with well-defined surface conditions, this statement is not true. There are minimum limit values below which breakage probability is zero. In fact, many practical glass usages have relied and do rely on this fact.

1.3 Ideal versus Practical Strength

The strength of glass calculated from its atomic bonds is extremely high.^{10,11} It might even reach 5 GPa. 1 GPa is one gigapascal, which equals 1000 MPa (megapascals) or 1000 N/mm² (Newtons per millimeter square). A rod of glass having this ideally high strength with a cross section of 1 cm² could carry a weight of about 40 metric tons. However, the practical strength is lower by orders of magnitude (see Fig. 1.3). The first effect that reduces this tremendous value by at least a factor of 5 is the presence of flaws in the atomic microstructure. The highest reduction, however, by a factor of 100 or more comes

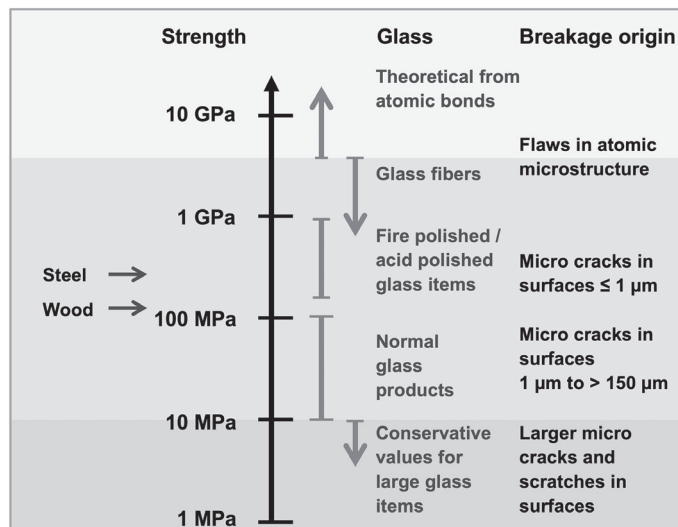


Figure 1.3 Typical strength ranges of glass items with different surface qualities. Strength means the minimum stress leading to breakage. All values are rough numbers not suitable for concrete designs. The indications for steel and wood serve for comparison, and that of wood relates to the strongest types. (Figure adapted from Ref. 25.)

from the presence of surface flaws. Between 100 MPa and 1 GPa, such flaws are about 1 μm deep or less. Going below 100 MPa in strength and approaching 10 MPa, the flaws become deeper—from a few microns to more than 100 μm .

If it is possible to avoid surface micro-cracks, glass can withstand extremely high tensile stress even in practical applications. Glass fibers with their surfaces directly protected after drawing have tensile strengths much higher than steel. This structure is widely used for composite materials, with glass fibers providing the desired high strength and the surrounding material protecting them against scratching.

Considering the strength of glass in practice means assessing its surface condition and especially the depth of its typical micro-cracks. It is all about maximum crack depths in tensile-stress-loaded areas. This holds only for glass items that are not prestressed for strength enhancement. With thermal and especially chemical prestressing, significantly higher strength can be achieved. However, with optical glass this is not possible because prestressing introduces large optical inhomogeneity due to birefringence. With extremely low-expansion glass ceramics, thermal prestressing is not possible because this requires a high coefficient of thermal expansion. Chemical prestressing is also not possible because it will warp precision faces. Therefore, this treatise deals only with non-prestressed glass items.

There are rule-of-thumb values for the strength of glass and glass ceramic items: for undamaged borosilicate glass items exposed to a normal working environment, a safe value for strength is 6 MPa. Glass ceramics, being somewhat stronger, can be used up to 10 MPa without special considerations if they do not show obvious serious surface damage. However, these are very low values excluding any applications with higher requirements. The purpose of this treatise is to show that applications with much higher loads are possible. Glass and glass ceramic should not be excluded from designs from the very beginning only based on these extremely low and pessimistic numbers.

1.4 Surface Condition: Micro-cracks

The strength of brittle materials is all about surface cracks. This holds for all materials resulting from casting processes such as glasses. Brittle materials produced using a sintering process are different. They usually break starting from volume flaws. Such volume flaws do not exist in molten and cast glass and glass ceramics. For determining the strength of glassy materials, the main task is to characterize surface conditions and their consequences with respect to breakage behavior.

Optical elements made from glass or glass ceramics usually have at least one polished face and ground lateral or back faces (see Fig. 1.4). Faces ground with diamond grains show many micro-cracks (see Fig. 1.5).

Chapter 2

Breakage Stress Measurement

2.1 General

The mechanical strength of a glass or glass ceramic type is not a property given only by the bulk material as defined by its chemical composition such as density or Young's modulus. Different surface conditions lead to large strength variations. Even for one single glass type, these variations can be larger than those among glasses with totally different compositions prepared with the same surface-generation method. In order to characterize strength, it is necessary to always specify material and surface condition in combination. A surface condition specification example for the glass ceramic ZERODUR[®] is "ZERODUR[®] D64 bonded diamond grain flat ground" and an example for the optical glass SCHOTT N-BK7[®] is "N-BK7[®] lapped with silicon carbide SIC 600 loose grain."

The first important task in breakage stress measurement is to prepare specimens that are typical for the surface condition being investigated. The production must be uniform for all specimens of a sample in order to obtain sufficiently reliable statistics.

The micro-crack distribution not only depends on grain size but also on additional parameters of the generation process. For diamond grain grinding, these parameters are the geometrical directions of tool rotation and movement with respect to the moving or static workpiece and the tool feed rate. For silicon carbide lapping, one will obtain different results if a batch of fresh silicon carbide grains is used versus an older batch, where originally larger grains have been reduced and equaled in size due to wear. Variations in the optical polishing process should not have considerable influence as long as the micro-cracks from the preceding grinding steps have been removed as is required in good polishing practice. With surface etching, the decisive influence is the ratio between the etched-off layer thickness and the maximum crack depth of the preceding grinding step. The etching agent's composition might also contribute to variation.

All subsequent statistical analysis, strength, and lifetime calculations are based on a model using one unique undisturbed statistical distribution

Chapter 3

Evaluation of Measurements: Weibull Distribution

3.1 General

The aim of the measurement evaluation is to derive a theoretical description for the breakage probability depending on the applied tensile stress. The description should be accurate enough to allow for predicting with sufficient confidence the breakage or stability for given practical conditions. At first glance, all breakage incidents seem to occur statistically. A closer look shows that there is also a range of deterministic elastic behavior as a reaction to tensile stress without any breakages. The general approach for the behavior of brittle materials under tensile stress loads consists of a stress range with a statistical breakage process described with a probability distribution and the low-stress range where no breakages occur at all.

The underlying statistical distribution for the breakage of brittle materials is the distribution of subsurface micro-crack depths (see Fig. 3.1). From 30- μm depth and upwards, the data follow an exponential distribution with an upper limit given by the finite force applied during grinding. The sharp decline towards small depths is an artifact. Most of the small cracks are not visible due to the surface roughness, which obscures them.

However, the exponentially falling micro-crack–depth distribution is not the statistical distribution that directly describes the breakage probability. This is because a breakage always starts from the deepest micro-crack present in a uniformly tensile-stressed surface. In a ground surface there is a huge number of micro-cracks. In D151 ground ZERODUR[®], there can be around 45000 micro-cracks per 2.54 cm², which is the size of the loaded area of the ring-on-ring test setup presented in the previous chapter. There will be a roughly estimated 200 micro-cracks of more than 100- μm depths in the tested area of one specimen. The deepest of them starts the breakage; for each specimen, its own deepest micro-crack starts the breakage. Therefore, the experimentally determined breakage probability distribution reflects the frequency distribution

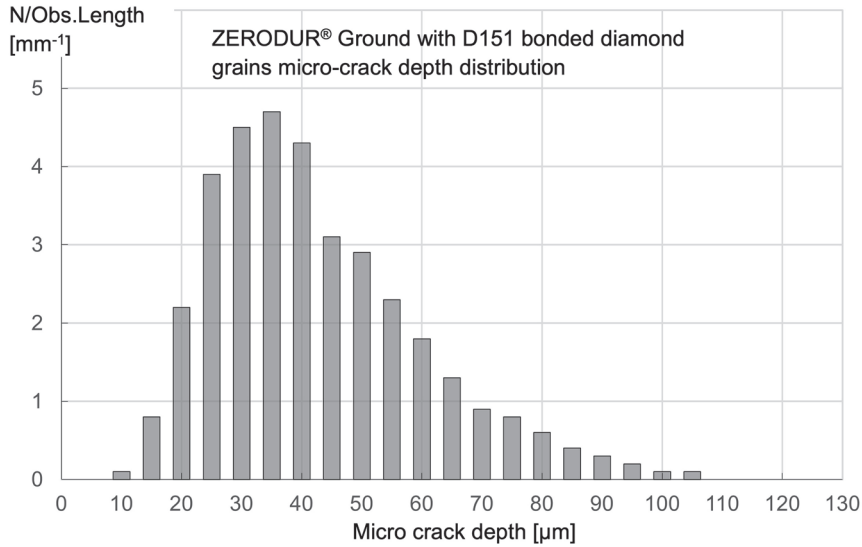


Figure 3.1 Histogram of micro-crack depths in a specimen of ZERODUR® ground with a D151 bonded-diamond grain tool. The number of micro-cracks is related to the observation length along the side view of the split specimen. For more details refer to Chapter 5.

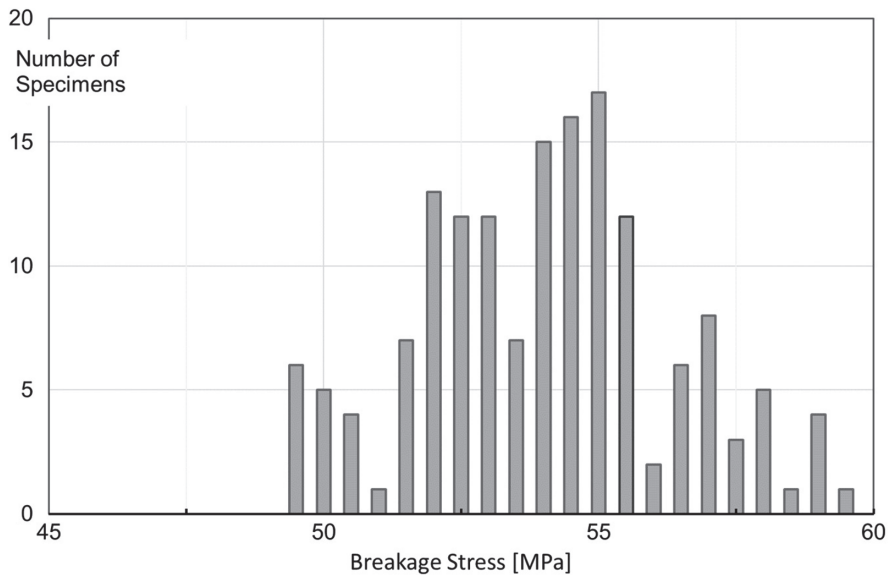


Figure 3.2 Histogram of the breakage stress frequency in a sample of ZERODUR® specimens ground with a D151 diamond grain tool.

of each deepest micro-crack per specimen in a sample of equally prepared specimens (see Fig. 3.2).

This distribution cannot be the normal Gaussian distribution because it presupposes that the single events contributing to the distribution are

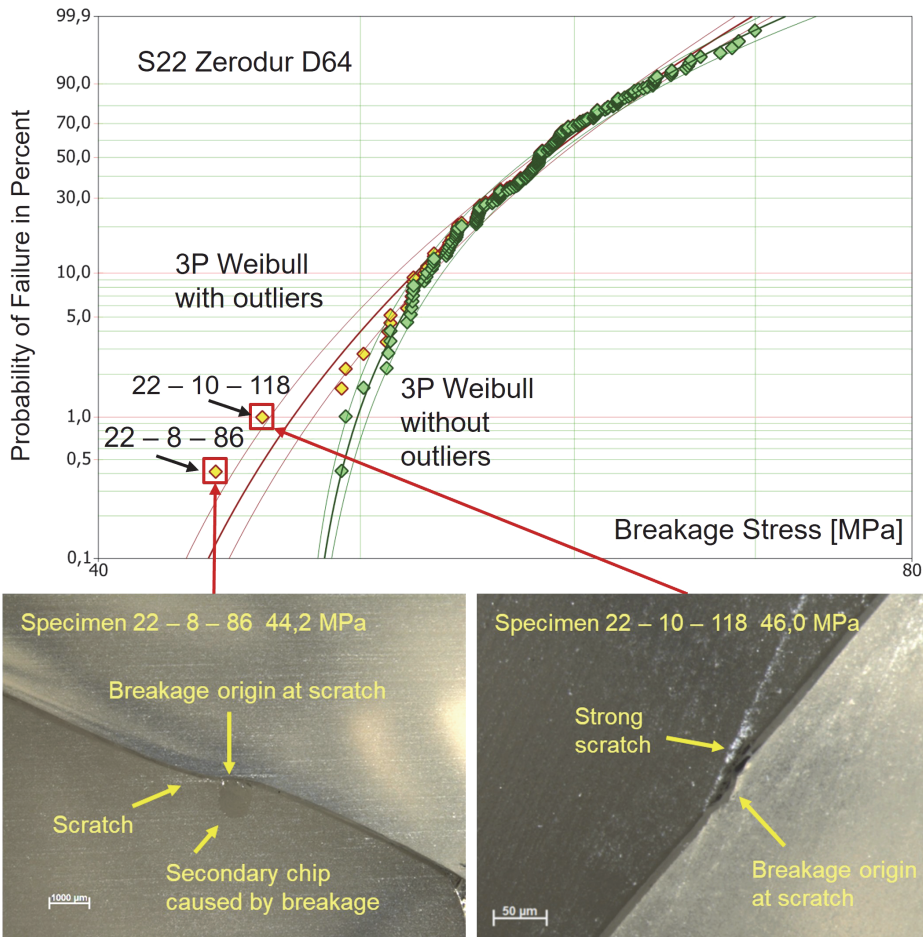


Figure 3.17 (top) Weibull plot of a sample of D64-ground ZERODUR® tiles (disk S22) fitted with and without two outliers. The lower images show the irregular breakage origins of the two tiles at strong scratches; these two tiles are not representative of the bonded-grain micro-cracks in the grinding process. (Lower images courtesy of SCHOTT AG.)

stress, specimens with the lowest values in an experimental sample should be examined very carefully.

Figure 3.17 gives another example where two outliers lower the threshold stress considerably when they are included in the sample. The irregular breakage origins at strong scratches can be clearly identified for the two outliers. (The cause of the scratches needs to be discussed separately.) The two outliers must be removed by any means from a distribution that represents the micro-cracks introduced by the bonded grains in the grinding process.

For practical surfaces, however, the possible occurrence of scratches must be checked and taken into account for surface qualification and strength

Chapter 4

ZERODUR[®]: Strength of Ground Surfaces

4.1 Introduction

Since 2007, SCHOTT has been performing strength measurement on ZERODUR[®] with much greater effort compared to earlier years.¹⁻⁶ An increasing number of applications needed reliable strength data for the mechanical loads occurring with them. An example for a high short-term load is satellite launch vibrations. Another application occurs with large segmented-mirror telescopes. Support and shape control elements bonded to mirror element back faces exert long-term loads. Such bonds must be tight for the total lifetime of the telescope. This might be up to 50 years. The initial reason the measurement campaign started in 2007 was for the design of ZERODUR[®] frames needed for the probe containers and the optical bench of the LISA Pathfinder gravitational wave detection experiment.

The strength data of ZERODUR[®] existing before 2007 were derived from samples with up to 20 specimens. The calculation of the admissible maximum stress with an accepted failure probability for a required lifetime was based on a two-parameter Weibull distribution fitted to the data (see Fig. 4.1). Along with some additional factors, the allowable breakage stress resulted from the intersection of the extrapolated fitted straight line with the acceptable level of failure probability. For a maximum failure probability of $1 \cdot 10^{-5}$, the calculation did not seem to be reliable enough due to the small statistical basis of only 20 specimens determining the position and slope of the fitted line. For ZERODUR[®] items with etched surfaces, the situation is even worse than for those with ground surfaces. The confidence bounds and the extrapolation range are even wider.

The target of the measurement campaign since 2007 was to re-measure strength with much better statistics with samples of sufficient size. Keeping costs within reasonable limits required a method for specimen production other than the one used in the past. The traditional way, the individual grinding of specimens in the laboratory workshop, was too expensive. The idea was to create many specimens in one common process in the production

Chapter 5

Micro-crack Depths

5.1 Introduction

The strength of brittle materials depends decisively on their surface conditions. Glass with a perfect surface can be extremely strong. It can withstand tensile stress up to 5 GPa. However, surfaces have imperfections resulting from processing or from wear. Point-like contact with material harder than the glass might introduce a wide variety of surface cracks during usage of glass items depending on the touch forces. Processing leads to a reduced variety of damages because of the common origin of surface cracks. In the following, only surface conditions of processed glass ceramic will be treated. One finds such surfaces, for example, at mirror side or back faces. Optically polished mirror faces have, by far, fewer surface imperfections if they were made according to the good polishing practice of removing all micro-cracks from the preceding grinding steps. Therefore, the ground faces are the weaker parts of the element compared to the polished faces. They set the limit of the overall strength of an optical component.

With optical materials, cutting and shaping are always grinding processes. Other cutting or shaping processes that work by introducing heat, e.g., laser cutting, are not allowed. They would result in local changes of essential material properties such as the coefficient of thermal expansion and the permanent internal stress, leading to impairment of their required high homogeneity.

Grinding is done using diamond or silicon carbide grains of different size distributions to adjust for the needed efficiency and surface quality. In any case, they introduce cracks, pits, and grooves (Fig. 5.1). Parts of the surface texture can be detected by surface touching measurement tools, examples of which are a mechanical stylus with a very fine tip or a focused laser beam (Fig. 5.2).

The recorded surface texture is commonly addressed as roughness. Contrary to other materials, in glass, micro-cracks continue into the bulk material below this roughness layer. They reach much deeper. This can amount to up to four to five times the value of roughness. This depends on the defined roughness quantity such as the peak-to-valley (P-V) roughness as in

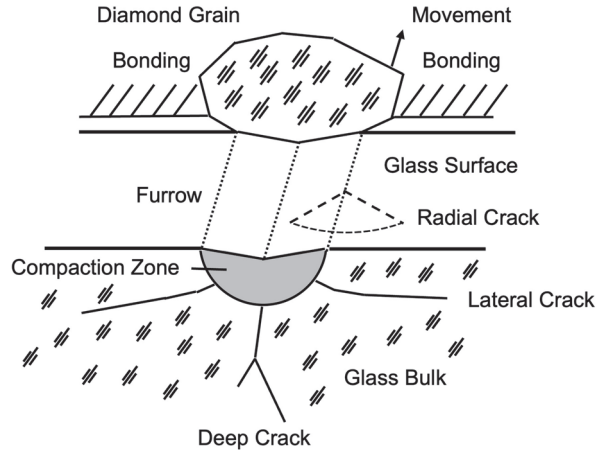


Figure 5.1 Glass grinding mechanism with scratching by bonded diamond grains. Lateral cracks enable removal of glass layers. (Figure reprinted from Ref. 16.)

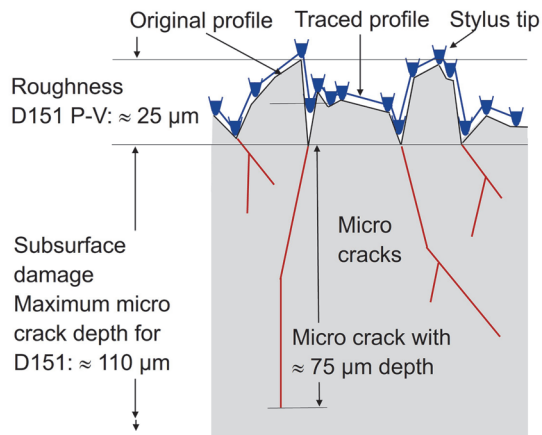


Figure 5.2 Schematic diagram of roughness and micro-cracks of brittle materials with example values of D151 ground ZERODUR®.

Fig. 5.2 or the P-V roughness mean of five sample surface profiles R_z as used by R. Jedamzik.¹ The micro-crack cleavage width becomes so small that a stylus or laser beam cannot follow it to find the location of the very tip. One essential problem in dealing with strength is that a certain part of the micro-crack extension is not measurable with the required accuracy and without destroying the surface condition. The other essential problem is finding the deepest micro-crack in a very large number of accompanying cracks.

The cracks in this sub-roughness layer are commonly called subsurface damage, abbreviated as SSD.

Subsurface damage influences not only strength but also other properties of optical elements. Micro-cracks might generate stray light and reduce laser

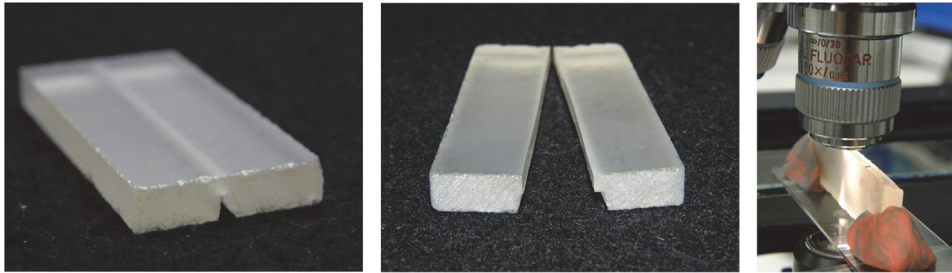


Figure 5.3 (left) $50 \times 20 \times 5 \text{ mm}^3$ specimen for direct micro-crack observation with a groove on the back side. (middle) Specimen broken from the back side, rendering two observation surfaces. (right) Microscopic investigation of a cracked face. (Figures adapted from Ref. 6.)

5.3 Micro-crack Appearance

Figure 5.4 shows an image of a ZERODUR[®] D151-ground surface along a length of about 2 mm. The roughness range is about $25 \mu\text{m}$. Isolated micro-cracks extend deeper into the material—in this figure, up to $100 \mu\text{m}$.

Figure 5.5 shows two enlarged views of D151-ground surfaces with micro-cracks more clearly visible. The image on the left shows two larger

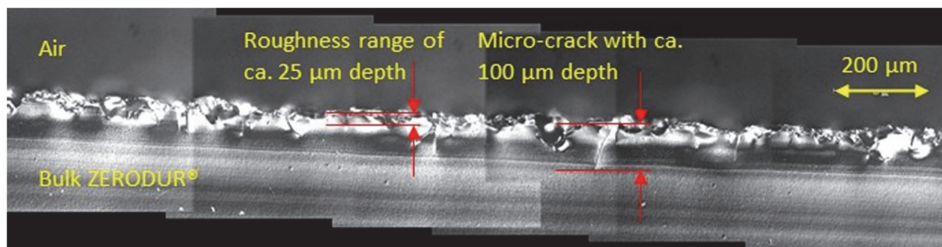


Figure 5.4 ZERODUR[®] D151-ground surface with roughness and isolated micro-cracks. (Figure reprinted from Ref. 17.)

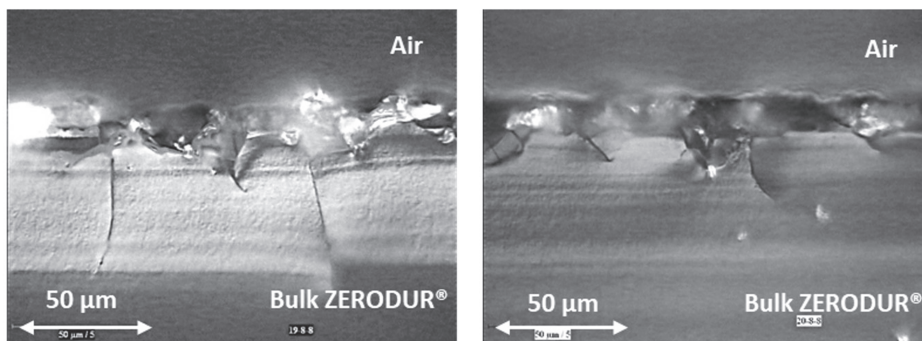


Figure 5.5 ZERODUR[®] D151-ground surface with roughness and isolated micro-cracks with larger magnification. Examples with (left) larger and (right) smaller micro-cracks. (Left image reprinted from Ref. 17; right image courtesy of SCHOTT AG.)

Chapter 6

Bending Strength of Etched ZERODUR[®]

6.1 Introduction

In Chapter 4 it was shown that ZERODUR[®] ground with diamond grains or lapped with silicon carbide grains is much stronger than thought in earlier times. The decisive influence on strength is the presence of micro-cracks in the surface and their maximum depth. Therefore, smaller micro-crack depths should lead to higher strength. This is confirmed by breakage stress samples prepared with smaller grains sizes, as the data presented in Chapter 4 show. The effect, in fact, is smaller than assumed. From D151-ground surfaces, strength increases only by about 40% with respect to D25-ground surfaces even though the maximum crack size reduction from 107 μm to 20 μm is more than a factor of five. This comparison relates to the breakage stress thresholds of 67.7 MPa (D25) and 47.3 MPa (D151) and the micro-crack depths displayed in Fig. 5.6.

Another way to reduce micro-crack depths or even remove them completely is etching of the surfaces. Before 2007 there was very little information available. Just three samples, two with 20 specimens each and preground with D64 bonded grains and one sample with lapped specimens, had been measured (see Fig. 6.1). The thicknesses of the etched-off layers were not known very accurately. They were not recorded and could be reconstructed only indirectly. For the sample with only seven specimens lapped with SIC 600, the etched-off thickness is not known at all.

Even from the small samples, the large leap in strength is clearly visible. Sample ZM D64 E99 with the etch depth of 99 μm extends to higher breakage stresses, but its minimum value lies very close to that of the other D64 sample Z D64 E71 with the smaller thickness of 71 μm etched off. The etched sample prelapped with the very fine-grain SIC 600 lies in the same range. Its width is much smaller and the minimum value lies considerably higher. The findings look plausible; however, statistics with 47 specimens in total is too poor for statements requiring higher reliability.

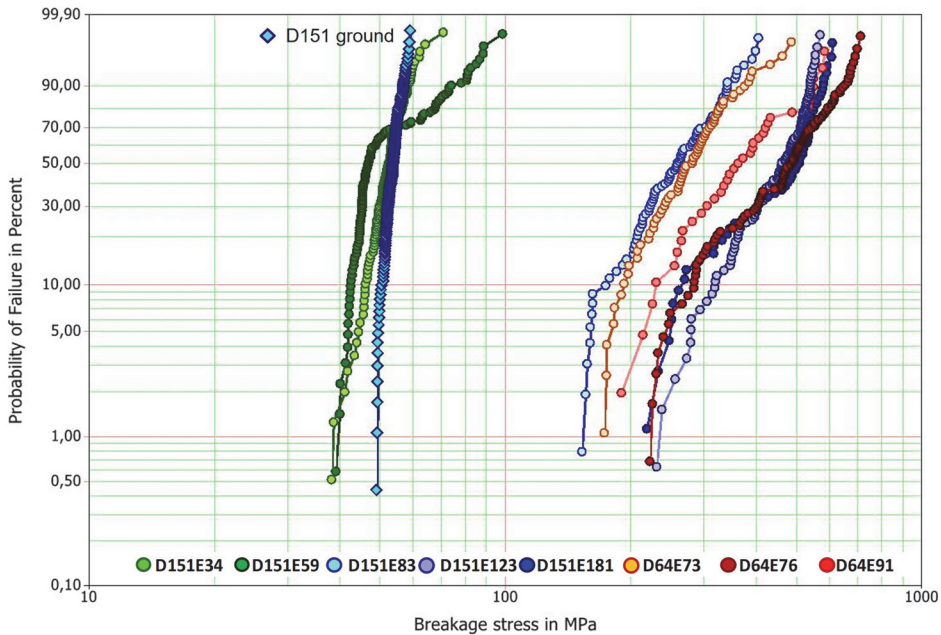


Figure 6.11 Weibull plot of ZERODUR® samples pre-ground with D151 and D64 bonded diamond grains and then etched. All data are as in Fig. 6.8, but with outliers removed. (Figure adapted from Ref. 7.)

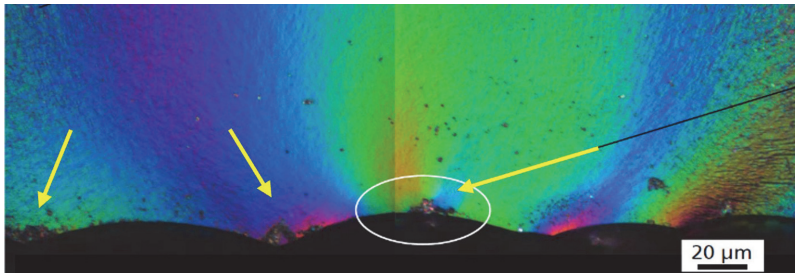


Figure 6.12 Micrograph of an etched tile cullet inside view with micro-damage on a fully etched surface. (Figure reprinted from Ref. 7.)

The only-ground surfaces are flat within the range of their roughness ($\sim 25 \mu\text{m}$ for the D151-ground surface shown in Fig. 6.2). For flat surfaces without holes, the tensile stress is uniform close to the surface.

The beginning etching leads to the creation of holes at the locations of micro-cracks. With etching times of 5 to 40 minutes, the holes become deeper ($45 \mu\text{m}$ to $35 \mu\text{m}$) than the peak-to-valley value of the roughness. Continuing the etching up to 60 minutes, there are no longer any holes, but shallow pits appear with depth values even below the original roughness.

Chapter 7

Strength Change with Time: Fatigue

7.1 Fatigue Mechanisms: Wear and Stress Corrosion

In the measurements for determining the breakage stress of ZERODUR[®] samples, the breakages occur a short time after loading the specimens. Breakage stresses for ground samples extend from 50 to 130 MPa and those for etched samples from 120 to 700 MPa. With the standard stress increase rate of 2 MPa/s, this corresponds to 25 s to 65 s and 60 s to 350 s. Load times for the practical use of ZERODUR[®] mirrors and components can be as short as 15 minutes for a rocket launch, but in most cases they will be years or even decades. To predict the behavior of the components for times with five to six orders of magnitude longer than the experimental loading times, fatigue mechanisms must be known as well as how they can be taken into account.

The strength degradation of glass items has two main causes. One is worsening of the surface condition due to wear. Contact with harder materials in the form ranging from bulky pieces down to dust grains during use and cleaning processes lead to more and possibly deeper micro-cracks in the surface than were present originally. This fatigue effect can be reduced or even avoided completely by protecting the optical elements' faces, for example, by making them inaccessible or by covering them. Cleaning must be done very carefully.

The other weakening cause is the growth of already existing subsurface micro-cracks under the influence of tensile stress. If tensile stress exceeds a threshold value, micro-cracks will start growing with an extremely low rate. If the stress remains in a range not too far above the threshold, the subcritical crack growth can go on for many years without leading to any breakage. For in-depth information, see the extensive reviews of Freiman, Wiederhorn, and Mecholsky¹ and of Ciccotti², both from 2009.

7.2 Subcritical Crack Growth: Stress Corrosion

The subcritical crack growth rate v depends not only on the tensile stress σ but also on the crack's depth a and a geometrical crack form factor f . These three

repetition was that this institute could provide a much wider range of the stress-increase rates that specifically extend down to 0.004 MPa/s. This is of high interest for predicting the behavior of ZERODUR[®] with long-lasting loads.

7.4 Derivation of the Stress Corrosion Constant versus Stress Increase Rate Equation

The relationship between the stress $\sigma_{B,r}$ at which a specimen with an initial micro-crack length a_i will break and the stress increase rate $\dot{\sigma}_r$ and its dependence on the stress corrosion constant n follows from the general crack growth law Eq. (7.2) with the definition of the stress intensity factor K_I in Eq. (7.1). A reformulation of both equations renders Eq. (7.3):⁸

$$dt = \frac{1}{A(\sigma\sqrt{af})^n} da \quad (7.3)$$

Integrating Eq. (7.3) for a constant stress increase rate $\dot{\sigma}_r$ [defined by Eq. (7.4)],

$$\sigma = \dot{\sigma}_r \cdot t, \quad (7.4)$$

from the initial state (index i) to breakage (index B),

$$\int_{t_i}^{t_B} t^n dt = \int_{a_i}^{a_B} \frac{1}{A\dot{\sigma}_r^n f^n} a^{-\frac{n}{2}} da, \quad (7.5)$$

renders

$$\sigma_{B,r} = \left[\frac{2(n+1)}{(n-2)A} \dot{\sigma}_r f^{-n} a_i^{-\frac{(n-2)}{2}} \right]^{\frac{1}{(n+1)}} \quad (7.6)$$

Logarithmizing Eq. (7.6) leads to a linear equation that allows one to determine the stress corrosion constant n from the slope of a straight line:

$$\log(\sigma_{B,r}) = \frac{1}{(n+1)} \log(\dot{\sigma}_r) + const. \quad (7.7)$$

Determining the stress corrosion constant requires measurement of breakage stress samples with different stress-increase rates. Long-term lifetime predictions rely on extrapolation over many orders of magnitude. From laboratory measurements done in half a minute to required lifetimes of 10 years, there are seven orders of magnitude to be overcome. Therefore, the stress-increase rates used for determining the stress corrosion constant should cover a wide range to obtain the best value that is valid in the long-term.

All tests presented below were performed according to the ring-on-ring method described in the European standard EN 1288-5 (see Chapter 2).

Chapter 8

Design Strength of ZERODUR[®] Including Fatigue: Lifetime

8.1 Introduction

There is a general reluctance to mechanical loading of brittle glass or glass ceramic items. The proverbial tendency to breakage, its sudden occurrence, and the total damage in many cases combined with the creation of razor blade sharp edges quite often prevent even considering the application of glass. On the other hand, brittle glass is used ubiquitously because of its unique properties such as its transparency, its beauty, and its optical properties. Common day experience shows that many glass items work for many years without any breakage, thus justifying their use. This supports the hypothesis that there is a minimum strength and a potential for higher loading of glass. The new deterministic approach introduced in 2012 removes uncertainties inherent with statistical methods.¹ It allows one to calculate minimum lifetimes for loaded glass or glass ceramic items, where statistical variations occur only above these values. The method outlined below includes fatigue caused by stress corrosion and can be successfully verified.²

The traditional failure probability calculation based on the two-parameter Weibull distribution predicts finite failure probability even for arbitrarily low bending stress.³ In this approach, the first question in strength design addresses which failure probability is acceptable. Hardly anyone is inclined to provide a specific number as an answer. The second and third questions relate to the size of the loaded area and the fatigue to be assumed. Usually, at each stage, the considerations made are conservative or even overly conservative. In the end, this adds up to a factor of safety that is much too large. The admissible stress will be reduced to minute values. The values will be hardly higher than the conservative rule-of-thumb values of 4–6 MPa for glass items and 10 MPa for glass ceramic items. Even for these values, according to the two-parameter Weibull distribution approach, failure probabilities exist that differ from zero. This does not really provide confidence in the material and therefore did not increase the number of glass applications with higher mechanical loads.

Table 8.1 Allowable constant tensile stresses for different required lifetimes of ZERODUR® surfaces ground with different grain sizes or etched in 50% relative humidity environment and measured with a constant stress-increase rate.

| $\dot{\sigma}_r$ [MPa/s] = 2 | | $n = 31$ | | | | | |
|------------------------------|-----------|----------------------|-------|-------|-------|--------|--------|
| Surface condition | | D151 | D46 | D35 | D25 | Etched | Etched |
| $\sigma_{T,r}$ [MPa] | | 47.3 | 51.0 | 57.4 | 67.7 | 120 | 200 |
| Lifetime | t [s] | $\sigma_{T,c}$ [MPa] | | | | | |
| 10 min | 6.000E+02 | 38.11 | 41.19 | 46.53 | 55.18 | 99.63 | 168.80 |
| 1 h | 3.600E+03 | 35.97 | 38.87 | 43.92 | 52.08 | 94.03 | 159.32 |
| 1 d | 8.640E+04 | 32.46 | 35.09 | 39.64 | 47.00 | 84.87 | 143.80 |
| 1 m | 2.678E+06 | 29.06 | 31.41 | 35.48 | 42.08 | 75.97 | 128.72 |
| 1 y | 3.154E+07 | 26.84 | 29.01 | 32.77 | 38.86 | 70.16 | 118.88 |
| 10 y | 3.154E+08 | 24.92 | 26.93 | 30.43 | 36.08 | 65.14 | 110.37 |
| 50 y | 1.577E+09 | 23.65 | 25.57 | 28.89 | 34.25 | 61.84 | 104.78 |

Figure 8.3 displays the lifetime of ZERODUR® items plotted against the applied constant stress for the stress corrosion constant $n = 94.5$, which is valid for an extremely dry environment of 5 ppm residual water, which in practice, means an application in vacuum.

Table 8.2 lists allowable breakage stresses for minimum required lifetimes from 10 minutes to 50 years for extremely dry environments. The measurements have been done with a constant stress increase rate of 2 MPa/s. The column “Etched 120” refers to a conservative minimum breakage stress for etched surfaces. The column “Etched 200” represents an optimally etched surface fulfilling three conditions: (1) the relative etch depth is greater than one, (2) etching started from a fine-ground surface without any scratches, and (3) no scratches occurred after etching.

8.4 Mechanical Loads Varying in Time

The lifetime model presented in the previous chapters is based on permanent loads of the same height throughout the total lifetime. There might be application cases where load variations with time could or should be considered. This applies to the presented model, too. However, before explaining this, it is worthwhile to check if this additional effort is really necessary.

Generally, one needs to distinguish the time during which the stress load lies below the subcritical crack growth threshold and the time when it is above that threshold. Only in the latter time will the strength degradation continue. Crack growth will follow stress variation according to the growth law [Eq. (7.2)]. This is difficult to account for in precise lifetime calculations because of the extremely high dependence of the crack growth velocity on

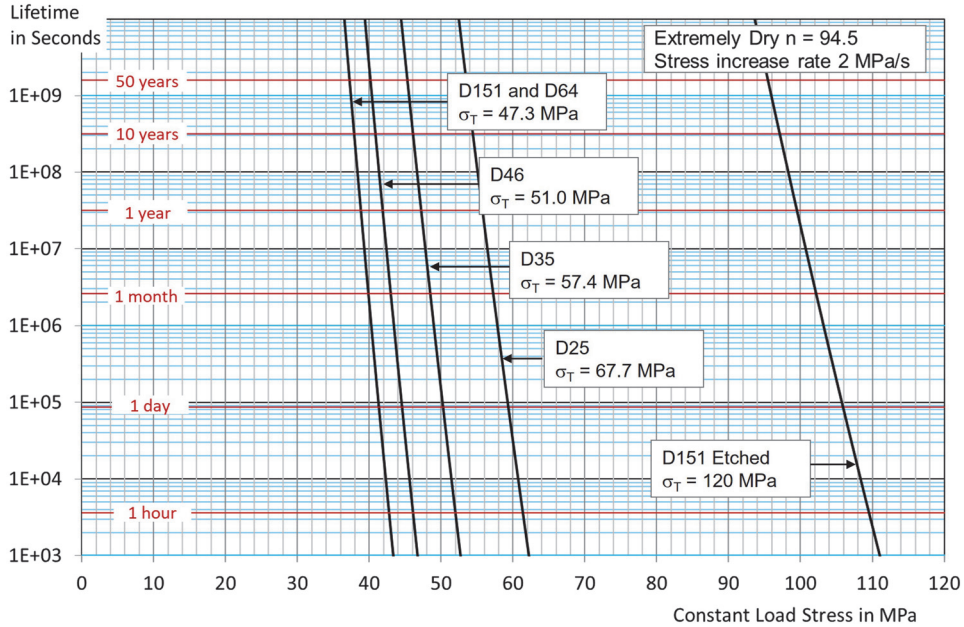


Figure 8.3 Lifetime calculations of ZERODUR® items prepared with five different grinding tools (D151, D64, D46, D35, and D25) and ground and then etched in a very dry environment (5 ppm residual water) ($n = 94.5$). The D64- and D151-ground surface curves coincide because the threshold stress values are almost identical. The short-term threshold stresses are given at the curves. The short-term minimum breakage stress for the etched surface curve is 120 MPa, a conservative estimate for sufficiently etched surfaces. (Figure adapted from Ref. 2.)

Table 8.2 Allowable constant tensile stresses for different required lifetimes of ZERODUR® surfaces ground with different grain sizes or etched in an extremely dry (5 ppm water) environment and measured with a constant stress-increase rate.

| $\dot{\sigma}_r$ [MPa/s] = 2 | | $n = 94.5$ | | | | | |
|------------------------------|---------|----------------------|-------|-------|-------|--------|--------|
| Surface condition | | D151 | D46 | D35 | D25 | Etched | Etched |
| $\sigma_{T,r}$ [MPa] | | 47.3 | 51.0 | 57.4 | 67.7 | 120 | 200 |
| Lifetime $t_{B,c}$ | t [s] | $\sigma_{T,c}$ [MPa] | | | | | |
| 10 min | 6.0E+02 | 43.56 | 47.00 | 52.96 | 62.58 | 111.60 | 187.00 |
| 1 h | 3.6E+03 | 42.74 | 46.12 | 51.97 | 61.40 | 109.50 | 183.49 |
| 1 d | 8.6E+04 | 41.32 | 44.59 | 50.25 | 59.37 | 105.88 | 177.42 |
| 1 m | 2.7E+06 | 39.85 | 43.00 | 48.46 | 57.25 | 102.10 | 171.09 |
| 1 y | 3.2E+07 | 38.82 | 41.89 | 47.21 | 55.78 | 99.47 | 166.68 |
| 10 y | 3.2E+08 | 37.89 | 40.89 | 46.07 | 54.44 | 97.08 | 162.67 |
| 50 y | 1.6E+09 | 37.25 | 40.19 | 45.30 | 53.52 | 95.44 | 159.92 |

Chapter 9

Bending Strength of Optical Glasses

9.1 Introduction

Normally, optical glass is not subject to strong stress loads. Therefore, its mechanical strength is usually not of special concern. In some circumstances, however, when optical elements will need to endure stress loads, considerations on how they can be prepared for higher loads might become necessary.

Such loads can be thermally induced stress as with optical elements close to strong lamps, optical systems in a hot environment, or high-optical-quality windows that are suddenly cooled (wind channel windows). Mechanical loads occur with vacuum windows, optical mirrors or prisms with high rotation speeds, rocket launch vibrations, harsh outdoor environments, and bonding of glass elements to glass or metal. These loads differ from each other not only with respect to their height but also to their duration. The main difference is between short-term loads, which last only seconds up to minutes such as rocket launches, and long-term loads, which extend over many years. This can be the case with bondings, for example. Glass withstands higher loads when the loads are short in duration. For long-lasting or even permanent loads, fatigue must be taken into account. The fatigue mechanism in glass, stress corrosion, is generally the same as might occur in glass ceramics. Above a minimum stress level, fatigue will gradually reduce strength with time. The presence of water, even only as humidity, enhances it.

SCHOTT published information and data for optical glass as early as 1991¹ and more recently in 2016.² In earlier times, the data given were the parameters of the two-parameter statistical Weibull distribution: the characteristic strength σ_c and the Weibull modulus or slope parameter λ . In the research done on the strength of the ultralow-expansion glass ceramic ZERODUR[®] presented in the previous chapters, the two-parameter Weibull distribution was found to be inadequate for elements with homogeneously ground or lapped surfaces.³ Moreover, it predicts design strength values that

Chapter 10

Recommendations for Optimizing and Maintaining the Strength of Glass Items

10.1 Introduction

The tendency of glass and glass ceramics to undergo sudden and catastrophic breakage is a great disadvantage of these materials. However, they have special properties that in many cases cannot be provided by other materials, such as extremely high transparency with precisely designable light deflection control or thermal expansion very close to zero. The use of these brittle materials is in many cases highly desirable or even without alternatives. In fact, they are widely used for very different purposes and under very different conditions. Applications with stress loads are also widespread. Glassy materials can endure such loads for long time periods when they are properly designed and handled. In the following discussion, some aspects partly relating to very different glass applications will be discussed that may be helpful for achieving adequate design and operation of glassy items under stress loads.

10.2 Risk Considerations

While considering failure probability of glass items, the first requirement arising is usually zero failure probability. Consequently, no glass items would ever have been used. Generally, this also applies for all other technical objects made from other materials. The question instead is which failure probability is acceptable. Even if the strength design was done very carefully by applying best methods and data, there is a residual risk due to imperfect realization of the product and unforeseen influences during operation. Therefore, in reality, any risk can never really be zero. For an overall design consideration, additional criteria should be taken into account, such as the worth of the glass item, the consequences of a failure of the system or of its operators or anybody else involved, reparability, and replaceability.

Chapter 11

Application Examples

11.1 Overview

An increasing number of cutting-edge technologies use ZERODUR[®] mirrors or structures capable of withstanding high mechanical loads. Not only do these mirrors and structures need to carry their own weight, but they must also endure additional loads caused by large and rapidly varying deformations or accelerations.¹ Satellite missions use very lightweight, delicate mirrors or support structures of complicated design that are subject to high mechanical loads from vibrations during rocket launch.

ZERODUR[®] has been successfully used in many space missions.^{2,3} In all cases, the mirrors or structures survived the launch accelerations without any problems. Three of these missions gave rise to breakage stress investigations in their preparation phase. The German x-ray satellite ROSAT was the first project to initiate such research around 1983. Six years later, NASA's larger x-ray satellite AXAF/CHANDRA led to continuation of the research. On this occasion, SCHOTT also included optical glasses in the mechanical strength investigations.

Finally, in 2007, a third ZERODUR[®] strength investigation began that used much larger samples in the preparation phase, this time, of the LISA Pathfinder mission.³⁻⁵ However, the strength requirements do not apply to space missions alone. There are also earth-bound applications that need to withstand higher mechanical loads, large segmented mirror telescopes, e.g., the European Extremely Large Telescope (ESO ELT), and optical system components in microlithography. The requirements for structure stability make the strength of ZERODUR[®] a key design parameter.

11.2 X-ray Satellite ROSAT

The core functional element of the German x-ray satellite ROSAT (Fig. 11.1) was a Wolter-type x-ray mirror assembly consisting of two times four cylinders [see Fig. 11.1 (*right*)]. The cylinders' length was 0.5 m and their diameters varied from 400 mm to 850 mm. The grazing-incidence x-ray reflecting surfaces had a super-polish with 0.2-nm residual roughness.^{6,7}

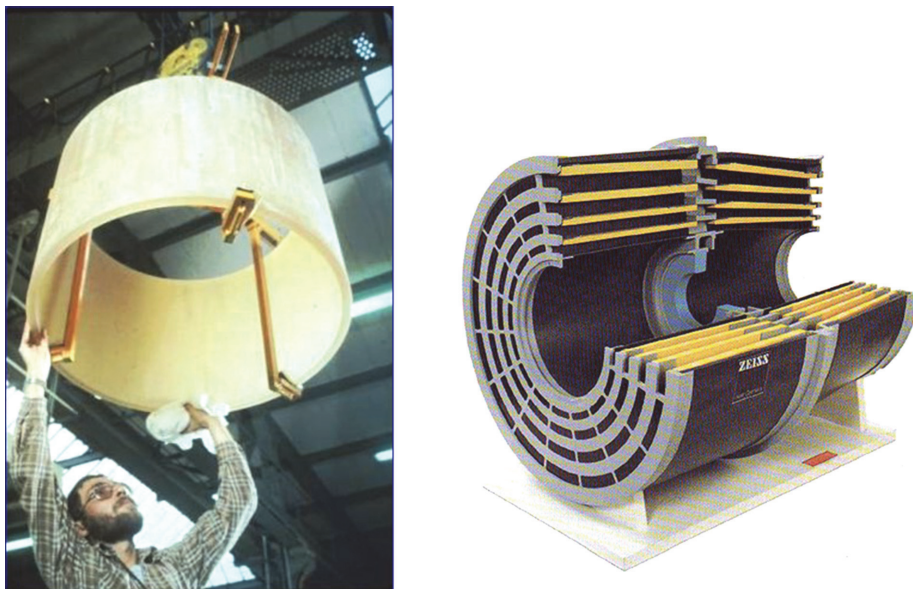


Figure 11.1 ROSAT x-ray mirror satellite. (*left*) ZERODUR[®] hollow cylinder blank for a mirror element. (*right*) Model of the Wolter-type x-ray mirror assembly. (Left image from SCHOTT AG and right image from a 1990 brochure of Carl Zeiss AG.)

Originally, the launch was scheduled to occur with a space shuttle. In the end, it occurred with a Delta II rocket on 1 June 1990. Because of this change, the satellite needed to endure a much higher acceleration load than previously planned. ROSAT's operation time spanned from 1 June 1990 until 12 February 1999—almost twice as long as expected.

11.3 X-ray Satellite AXAF/CHANDRA

The Wolter x-ray telescope of the CHANDRA satellite [see Fig. 11.2 (*left*)], formerly named AXAF, consists of two times four hollow cylindrical mirror elements made from ZERODUR[®]. The conical shells were drilled out from massive cast blanks [see Fig. 11.2 (*right*)]; they are thin walled (around 20 mm in thickness) and 1 m high [see Fig. 11.3 (*left*)]. The diameter varies from 0.6 m to 1.2 m.⁸ The cylinders were polished to extremely high quality and nested into each other [see Fig. 11.3 (*right*)].

On 23 July 1999, CHANDRA was launched into orbit with the space shuttle Columbia. Not only did the delicate, hollow cylinders need to survive the launch accelerations, but before the launch, they also needed to withstand a considerable number of transports and handlings in the preparation phases of polishing, coating, and integration.

Ever since its beginning, CHANDRA's performance was and is of unique quality.⁹ The observatory has surpassed its scheduled lifetime of 5 years by



Peter Hartmann received his Doctorate in Physics in 1984 from the University of Mainz, Germany. His thesis was on scintillation glasses made at the nuclear physics department of the Max-Planck-Institute for Chemistry in collaboration with Schott Glaswerke. In 1985, after serving as head of a geometrical metrology group in the automotive industry, Dr. Hartmann joined the optics division of Schott. Since then, he has been responsible for quality assurance, metrology development, and advising customers on optical glasses and the zero-expansion glass ceramic ZERODUR[®]. He has been involved in projects such as extremely high-quality optical glass for i-line microlithography and mirror blanks for large astronomical telescopes (Keck I and II, CHANDRA, ESO-VLT, GRANTECAN, ESO-ELT, LISA Pathfinder, and several 4-m telescopes). Since 2007, he has been the Director of Marketing and Customer Relations of Advanced Optics and Principal Scientist at SCHOTT AG until his retirement in 2018.

Dr. Hartmann served on the Board of Directors of SPIE from 2011 to 2013 and was active in international standardization as a convener of the ISO working group for optical materials. He was a member of the board of the Optics and Photonics Cluster OPTENCE, Hesse/Rhineland-Palatinate, Germany, and of the Board of Trustees of the Max-Planck-Institute for Astronomy, Heidelberg, Germany. He is a Fellow of SPIE and the author of *Optical Glass* (2014).